

CAAP 2019-2020 Annual Report

Date of Report: Oct 19th 2020

Prepared for: *U.S. DOT Pipeline and Hazardous Materials Safety Administration*

Contract Number: 693JK31850008CAAP

Project Title: Fluorescent Chemical Sensor Array for Detecting and Locating Pipeline Internal Corrosive Environment

Prepared by: Dr. Ying Huang, Dr. Wenfang Sun, and Dr. Hao Wang

Contact Information: Dr. Ying Huang, Email: ying.huang@ndsu.edu, Phone: 701.231.7651

For quarterly period ending: Oct 10th 2020

Business and Activity Section

(a) Contract Activity

Discussion about contract modifications or proposed modifications:

None.

Discussion about materials purchased:

None.

(b) Status Update of Past Quarter Activities

None.

(c) Cost share activity

Tuition for two graduate students with \$5,252 of cost share in this quarter.

(d) Annual Progress Summary

During Sep 2019 to Oct 2020, we made efforts working on three tasks: Task 2.1 and Task 2.2 of Task 2 (Development of Fluorescent/Colorimetric Chemical Sensor Array for Internal Corrosive Water Detection), successfully designed the sensors for Fe²⁺, Fe³⁺ and S²⁻ ions and sensitivity tests were performed with the development of color maps for concentration measurements from the sensor array; Task 3 (Corrosion Model for Corrosion Prediction), corrosion prediction model was selected and laboratory tests to obtain the influences of Sulfur on the corrosion rate tests were conducted; Task 4 (Feasibility Study of Field Installation and Inline Inspection Tools Integration), the pipeline robot were assembled and demoed for operation for the further detection tests. The detail findings are as below.

1. Background and Objectives (2019-2020)

1.1 Background

This project is designed to develop passive colorimetric/fluorescent chemical sensor array for locating and detecting corrosive water inside pipes. Inside the pipelines, the transported crude oil may include a hot mixture of free water, carbon dioxide (CO₂), hydrogen sulfide (H₂S) and microorganisms. The different chemical components inside oil/water environment such as HCO₃⁻ / CO₃²⁻, Fe³⁺, S²⁻, H⁺ or pH may result in different internal corrosion mechanisms, such as sweet corrosion or sour corrosion. The passive colorimetric sensor array to be developed in this project is intended to detect the concentration changes of the five above mentioned important chemical species in the internal oil/water environment of the pipeline and use these detected environmental data to predict the internal corrosion progressing of pipelines.

1.2 Objectives during 2019-2020

During 2019-2020, the major objectives are to 1) develop the chemical sensor array for detecting Fe²⁺, Fe³⁺ and S²⁻ ions and calibrating their sensitivity, accuracy, resolution, and repeatability with laboratory tests in addition to the development of gradient color maps (code) for the determination of the ion concentrations quantitatively; 2) select and calibrate the corrosion prediction model with various internal corrosion environments considered such as S²⁻ which can be used to develop further application of prototype models and verification along with parameter analysis; 3) demonstrate feasibility of integrating the sensor with LIL tools in laboratory environments; and 4) mentor, train, and outreach to broad students audience.

2. Results and Discussions

2.1 Summary of Quarter 5 (Oct 2019-Jan 2020)

In this quarter, we selected and tested three different porous polymeric materials, including PMMA (poly(methyl methacrylate) Isotactic), CA (cellulose acetate), and PMMA/CA polymer films) as a sensor film matrix for Fe³⁺. Figure 1 shows the test results for PMMA film, Figure 2 shows the results for CA and PMMA/CA film. The comparison between the three different polymer indicated that the PMMA/CA film out performed the other two films and is selected as a matrix for future chemical sensors in this project.

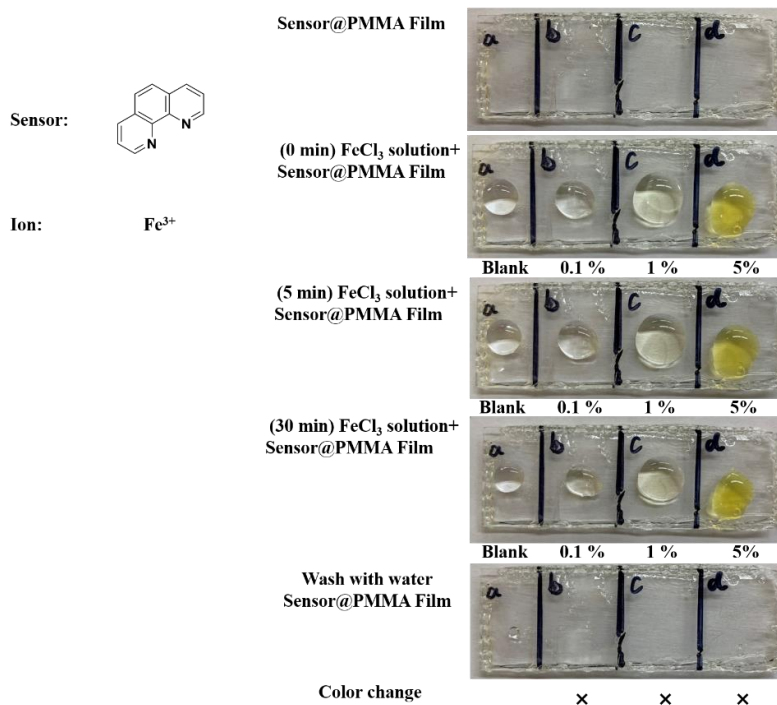


Fig. 1. Phenanthroline Sensor in PMMA film on glass substrate for detecting Fe³⁺

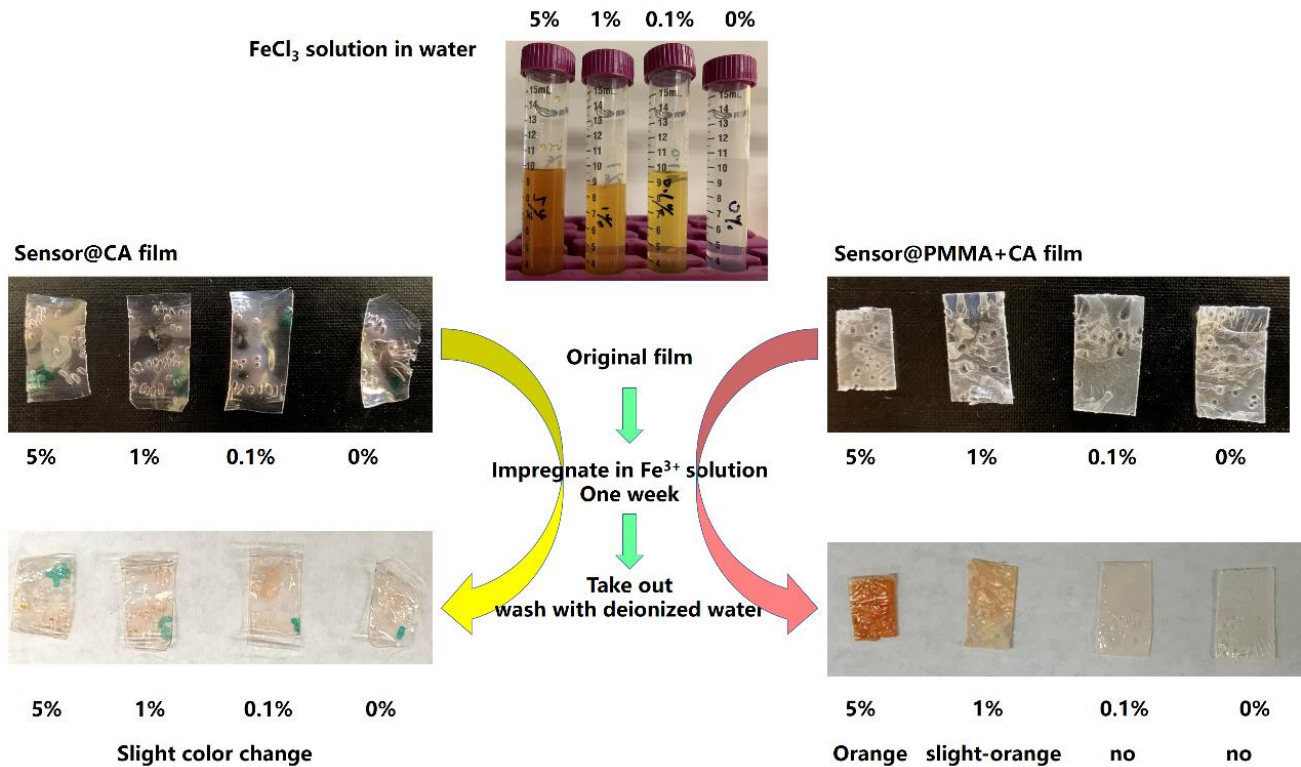


Fig. 2. Detecting Fe^{3+} in CA and PMMA/CA films with embedded sensors.

Whether the sensor film can survive the flow of oil/gas inside the pipe is of interested of this project, in this quarter, simulation using ANSYS was performed using 2D and 3D models. The comparison between the results from the 2D and 3D models showed that the 2D is more conservative and has less computation time, which was used for simulation. Figure 3 shows the simulated force on the sensor film from the model analysis. The total force on the sensor was about 8.23N for condition with the flow velocity of 0.5 m/s and the volume fraction water/oil of 60%.

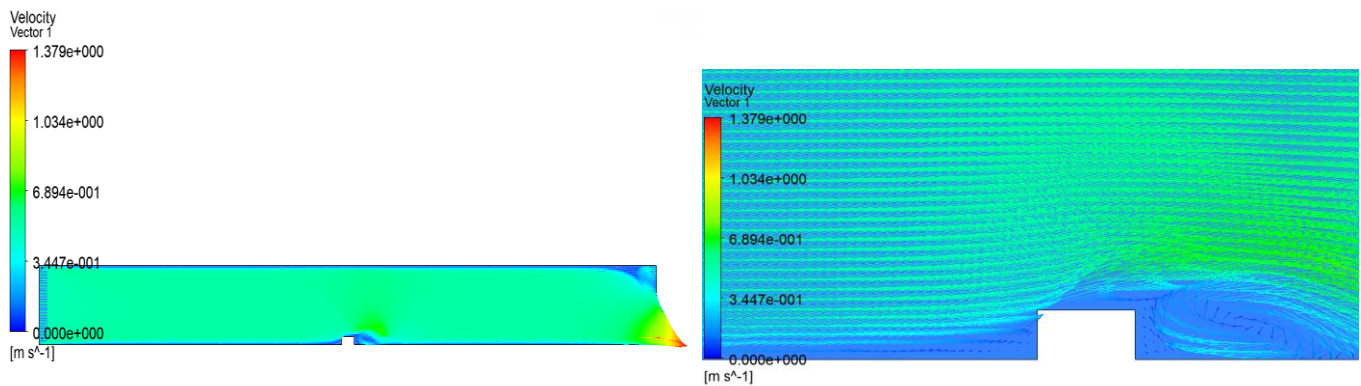


Fig. 3. Velocity vector around the sensor

To test the survivability of the sensor film and the impact of cleaning service on the color changes of the sensor film, a laboratory test of a simulated passage of a cleaning pig was performed in laboratory on samples without and with dipped into gasoline. Figure 4 shows the visual inspection of the samples after dipped into gasoline and after cleaning pig passed. Based on the test results, the following findings can be summarized:

- 1) The developed PMMA/CA sensor film can survive gas/oil in atmospheric condition;

- 2) The color change stayed unchanged after immersing the sensor film in gas/oil in atmospheric condition, indicating that no cleaning service is needed for the application of the detection of color changes of the sensor film;
- 3) The attached sensor film maintained their physical body intact under mechanical scratching from the rubber disk, indicating good physical stability to survive cleaning activities;
- 4) The cleaning process did not disturb the color change of the sensor film, showing the sensor film could survive and maintain functional when a cleaning/inspection pig passing.



(a) Attached sensor film after test without gasoline

(b) Attached sensor film after test without gasoline



(c) Attached sensor film after test with gasoline

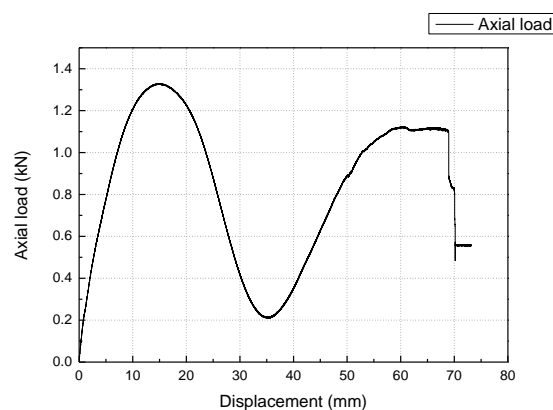
(d) Attached sensor film after test with gasoline

Fig. 4. Sensor's performance in service conditions

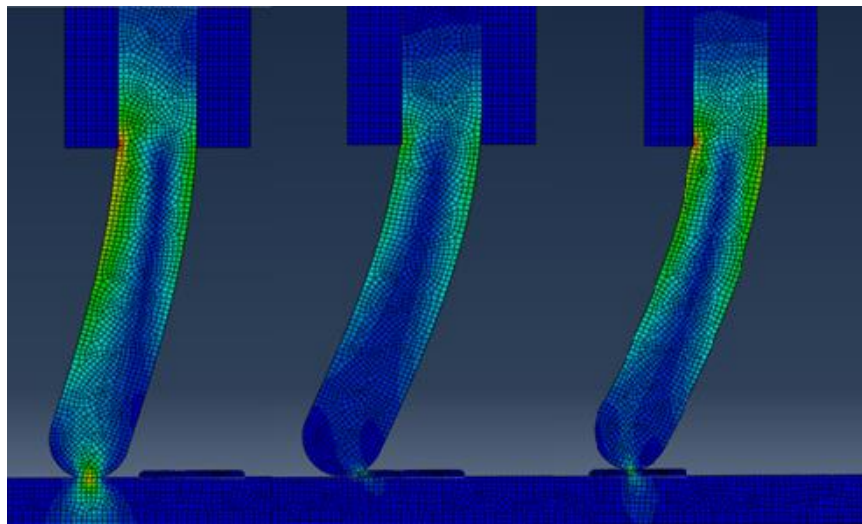
To further test whether the sensor can survive or need a cleaning service, the first series of the tests was conducted under atmospheric/oil condition as shown in Figure 5 (a). The maximum load tested is 630 N (Figure 5 (b)). The experimental tests in the previous report indicated that 540 N load was detected when disk went through the pipe without sensors. Thus, 90 N of the axial load was induced by the presence of sensor. This means the sensor carried a force of 100 N when the disk passed through the sensor. After acquiring all the parameters needed, the stress in the sensor under experimental condition (without gasoline) is 3.00 Mpa as calculated, which shows well correspondence with the simulated stress result (3.023 MPa) in Figure 5(c).



(a) Test setup



(b) Load-displacement curve of sensor film immersed in gasoline



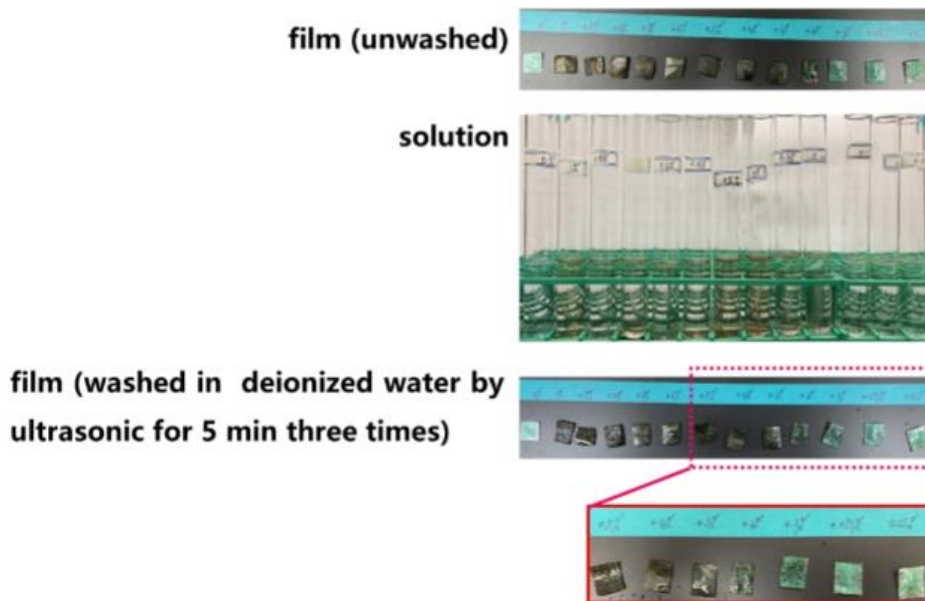
(c) Simulation results using ANSYS

Fig. 5. Survivability tests of sensor array

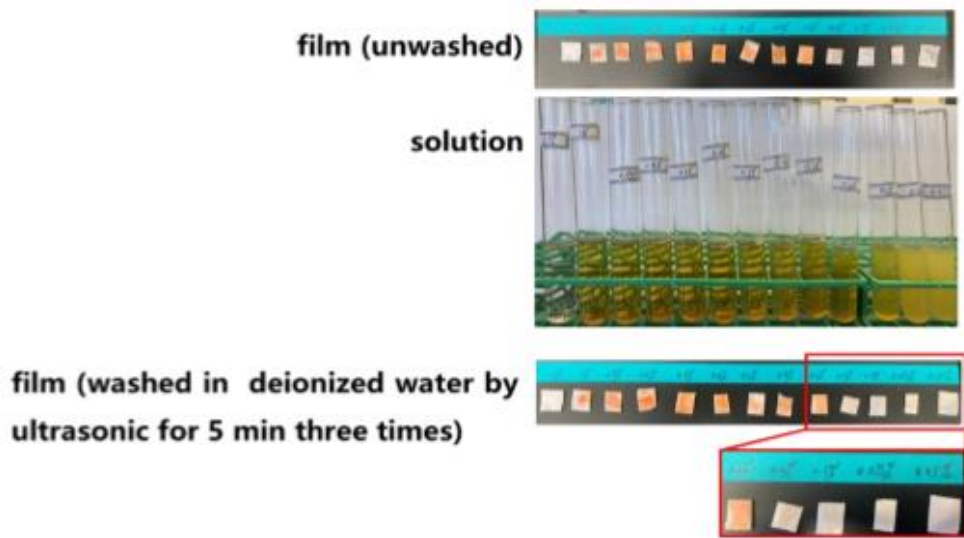
In addition, the corrosion prediction models were reviewed and the modified TJ model, a specific value of the corrosion rate under CO_3^{2-} condition can be calculated by measuring the concentration of Fe^{2+} and CO_3^{2-} ions inside the pipes. With the testing results from the developed sensors in this study, the sensitivity of the sensors can show the relationship between the indicating color and the concentration of the Fe^{2+} and CO_3^{2-} ions inside the pipes. The correlation between the ion concentrations to the corrosion rate can then be built, so that the definition of corrosion monitoring as well as protection can be established.

2.2 Summary of Quarter 6 (Jan 2020 to April 2020)

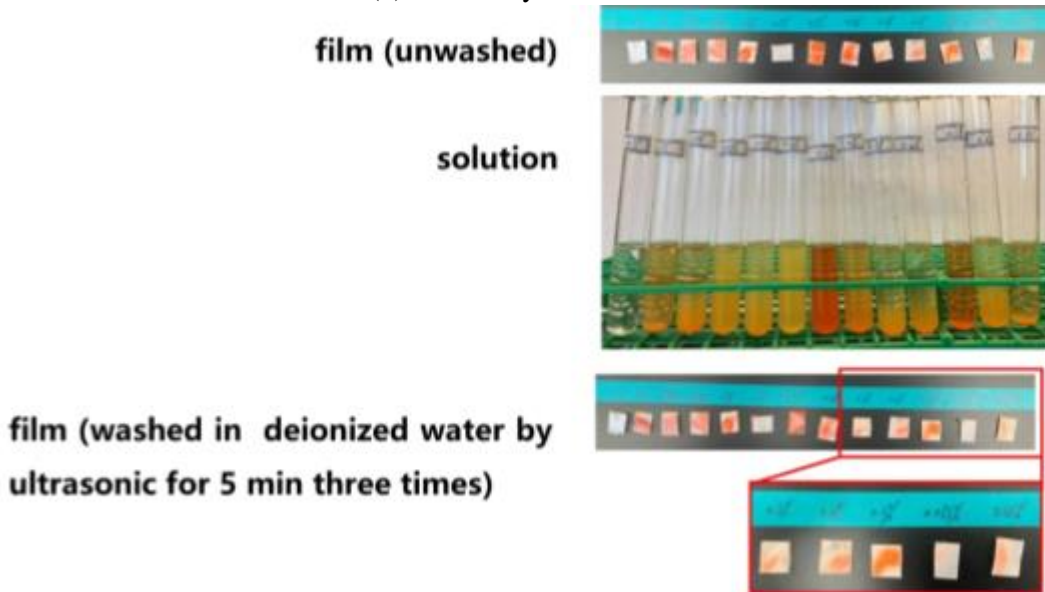
With the selected PMMA/CA sensor film, in this quarter, sensitivity tests were performed on the S^{2-} , Fe^{3+} , and Fe^{2+} ions as shown in Figures 6 (a, b, c).



(a) Sensitivity test on S^{2-}



(b) Sensitivity test on Fe^{3+}



(c) Sensitivity test on Fe^{2+}

Fig. 6. Sensor film of sensitivity tests on S^{2-} , Fe^{3+} , and Fe^{2+} ions

Based on the color changes, quantification is conducted in this quarter to form a base of establishing corrosion model according to the sensors' responses to target components of S^{2-} , Fe^{3+} , and Fe^{2+} ions in pipelines. International Commission on Illumination (abbreviated as CIE from its French title) stipulates that the wavelengths of the three primary colors of red, green and blue are 700nm, 546.1nm, and 435.8nm, respectively. When the ratio of the three-fundamental color changes, different color of light with different wavelength can be achieved. The corresponding test method is called color matching, and the amount of each color of red, green and blue by unit is called tristimulus value. To a certain color with a certain wavelength, the matching equation can be expressed as Eq.1:

$$C_o = R(R) + G(G) + B(B) \quad (1)$$

In the formula, C represents the color to be matched; (R), (G), and (B) represent the unit quantities of the three primary colors of red, green, and blue which are mentioned above; R, G, and B are the red, green and blue colors required to match the color to be matched, which are tristimulus values; and "o" means visually equal, that is, color matching. By using this method, any visible color or light can be described as a mixing of the identified RGB color.

The CIE-RG chromaticity diagram does not reflect the change of color brightness, but only expresses the range of color gamut. The spectral tristimulus value of the CIE-RG system can be obtained from experiments. It can be used for color measurement and calibration and chromaticity calculation. However, the negative portion of the diagram had made it inconvenient and unintelligible for practical use. Therefore, in 1931, CIE recommended a new international colorimetric system, namely CIE-xyz system, which is also known as the xyz international coordinate system. For the CIE-xyz system for its chromaticity diagram, it uses mathematical methods to select three ideal primary colors instead of the actual three primary colors, so that the spectral tristimulus values and chromaticity coordinates r , g , and b in the CIE-RG system become positive. After mathematical transformation, the relationship of the two-color systems and the two coordinate systems are shown in Eq. 2 and Eq. 3, respectively:

$$\begin{aligned} X &= 0.490R + 0.310G + 0.200B \\ Y &= 0.177R + 0.812G + 0.011B \\ Z &= 0.010G + 0.990B \end{aligned} \quad (2)$$

$$\begin{aligned} x &= (0.490r + 0.310g + 0.200b)/(0.667r + 1.132g + 1.200b) \\ y &= (0.117r + 0.812g + 0.010b)/(0.667r + 1.132g + 1.200b) \\ z &= (0.000r + 0.010g + 0.990b)/(0.667r + 1.132g + 1.200b) \end{aligned} \quad (3)$$

Therefore, as long as the chromaticity coordinates r , g , and b of a certain color are known, we can find their chromaticity coordinates x , y , and z in the newly identified three primary colors xyz color space. Based on Equation (2) and (3), the represented color for each concentration can be shown in Table 1 for S^{2-} and Fe^{3+} ions for detailed analysis.

Table 1 Representative color under Fe^{3+} and S^{2-} environment

Concentration	Fe^{3+} Segment outlook	Fe^{3+} Representative color	RGB code	Yxy code	S^{2-} Segment outlook	S^{2-} Representative color	RGB code	Yxy code
0.00%			255, 255, 245	99.373, 0.31852, 0.33861			161, 205, 197	55.269, 0.28609, 0.33929
0.05%			225, 220, 207	71.699, 0.32508, 0.34325			146, 171, 155	37.603, 0.30361, 0.35310
0.075%			238, 233, 215	81.362, 0.32767, 0.34775			156, 168, 145	37.117, 0.32130, 0.36333
0.1%			234, 220, 205	73.088, 0.33312, 0.34513			147, 164, 151	34.988, 0.30807, 0.34891
0.2%			253, 218, 207	75.533, 0.34625, 0.34035			113, 122, 104	18.429, 0.32219, 0.36500
0.3%			253, 214, 200	73.148, 0.35213, 0.34353			112, 113, 91	16.010, 0.33893, 0.37487
0.4%			234, 191, 172	47.504, 0.38874, 0.35959			120, 117, 101	17.655, 0.33610, 0.36060

0.5%			230, 186, 164	57.735, 0.36425, 0.35044			123, 113, 90	16.760, 0.35576, 0.37455
0.6%			239, 180, 153	53.296, 0.38875, 0.35927			111, 104, 82	13.890, 0.35314, 0.37647
0.7%			242, 136, 95	37.317, 0.47333, 0.37192			132, 122, 96	19.670, 0.35649, 0.37726
0.8%			240, 107, 70	29.488, 0.52194, 0.36384			120, 95, 69	12.608, 0.39244, 0.38318
0.9%			249, 143, 105	40.810, 0.46436, 0.36838			104, 82, 63	11.487, 0.37485, 0.40247
1.0%			247, 152, 116	43.496, 0.44555, 0.36744			88, 76, 57	7.539, 0.37062, 0.38029

In addition, for the stress analysis under cleaning activities, a sensitivity test on the influence of membrane thickness is needed to provide a deep view of thickness optimization using laboratory tests using the same setup as in Figure 5. Figure 7 shows the stress induced by friction in polymer membrane with sensor film thickness between 0mm to 6mm. It can be seen that the stress increases rapidly in two sections, which is 0.5mm to 2mm and over 3.5mm. So, for the survivability concern, the recommended thickness of the sensor base is less than 3.5mm, so that the stress in sensor can be controlled below 2.56 Mpa.

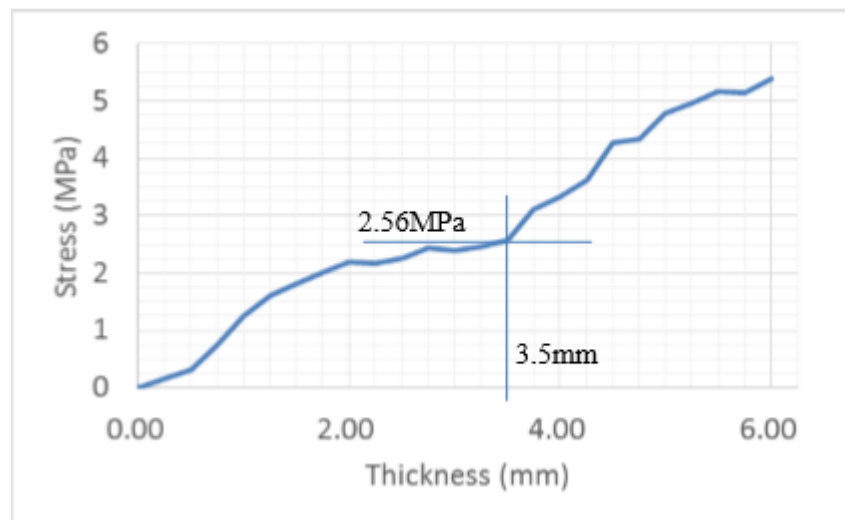


Fig. 7. Stress-Thickness curve of polymer membranes

2.3 Summary of Quarter 7 (April 2020 to July 2020)

In this quarter, to search for a reference of the empirical Corrosion Rate (CR) model, literature review work has been done to summarize previous research on applicable models on our target agent S^{2-} . Accordingly, further application of prototype models and necessary experimental tests on specific parameter determination can be done. In addition, to integrate the majorities of possible corrosive agents, a better understanding of the co-work mechanism between S^{2-} , CO_3^{2-}/HCO_2^- , and $pH(H^+)$ is also

considered. Based on the literature review, a summarized global CR prediction model can be formulized for future laboratory experiments.

2.4 Summary of Quarter 8 (July 2020 and Oct 2020)

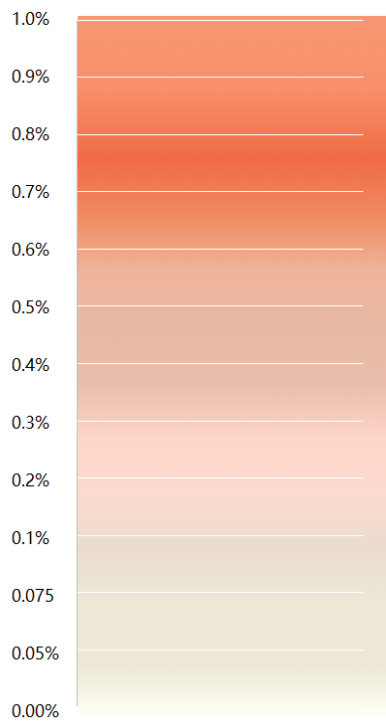
In this quarter, the detailed sensitivity tests of Fe^{3+} and S^{2-} ions for Task 2.2 were finalized with the development of gradient color maps in addition to a specified color code for the determination of the ion concentrations quantitatively. For task 3, in order to find a reference of the empirical Corrosion Rate (CR) model, potential-dynamic tests were conducted on our target agent S^{2-} . The resulted Tafel figures were used to calculate the corresponding corrosion rates under different S^{2-} concentration environments, which can be used to develop further application of prototype models and verification along with parameter analysis. Thus, a summarized global CR prediction model can be formulized according the research objectives within the project in next two quarters. For Task 4, during this quarter, demo inspection tools were assembled and its feasibility tests were performed.

2.4.1 Calibration of the Fluorescent/colorimetric Chemical Sensor Array (Task 2.2)

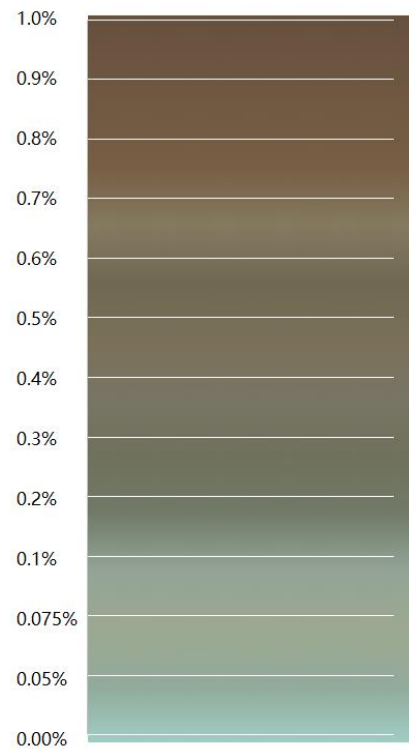
In previous quarterly reports (Quarterly Report #6), experimental sensor sensitivity tests have been conducted under Fe^{3+} and S^{2-} ion environments. The color change and the code in RGB were recorded as shown in Table 1. Table 1 showed the individual correspondence relationship between the concentrations of the ions and the specific colors. Based on Table 1, a full color map along with the development curve of each color component were developed in this quarter.

The individual representative colors at each concentration level in Table 1 can be transferred to expanded continuous color development maps using Photoshop as shown in Figure 1 (a, b) for Fe^{3+} and S^{2-} ions. The gradient color maps in Figure 1 were developed by extracting the representative colors under each concentration environment, which expanded the color on each concentration level to a full coverage of concentrations between 0.00% and 1.00%. Therefore, the developed gradient color maps in Figure 1 can be used to identify the concentration levels measured from the chemical color reactions of the developed sensor array for both Fe^{3+} and S^{2-} environments.

To further numerically quantify the color changes detected from the sensor array, the detected colors were divided into optical components using the RGB and Yxy theories. Figure 2 (a~d) show the individual developments of the optical components RGB and Yxy for both Fe^{3+} and S^{2-} ions. Based on Figure 2, detailed color characteristics can be detected for better utilization of the gradient maps. For each color, the color code represents the emerged environment with particular ion concentration. Thus, the sensor can detect the targeted ion concentrations with numerical quantification. A potential improvement in future quarters of the Gradient Color Maps and their corresponding color codes is to smooth the transition as the concentration gradually grows up for a more natural color diagram in Figure 1.

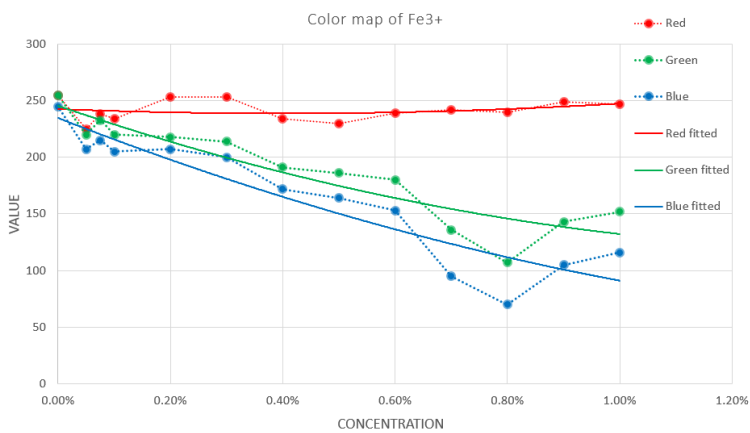


(a) Gradient Color Map of Fe³⁺ sensor response

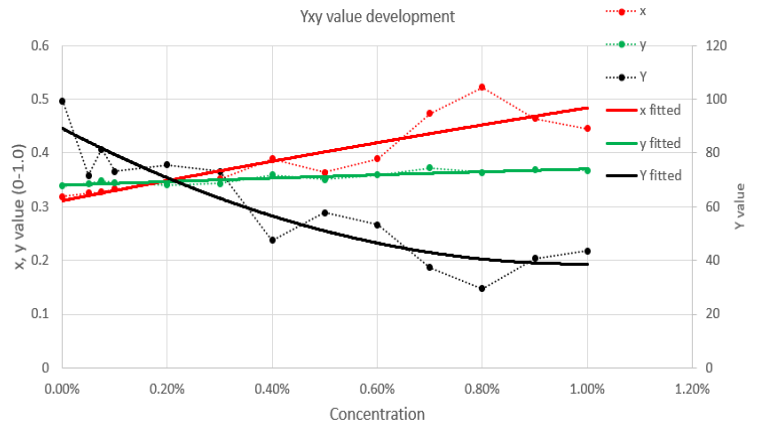


(b) Gradient Color Map of S²⁻ sensor response

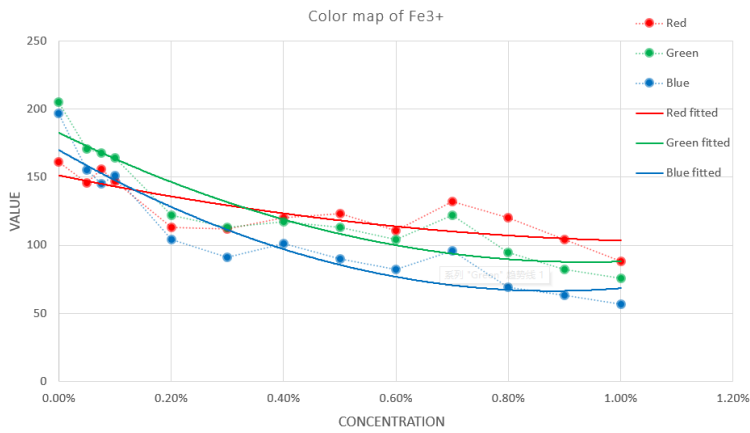
Figure 1 Gradient color chart of sensor response



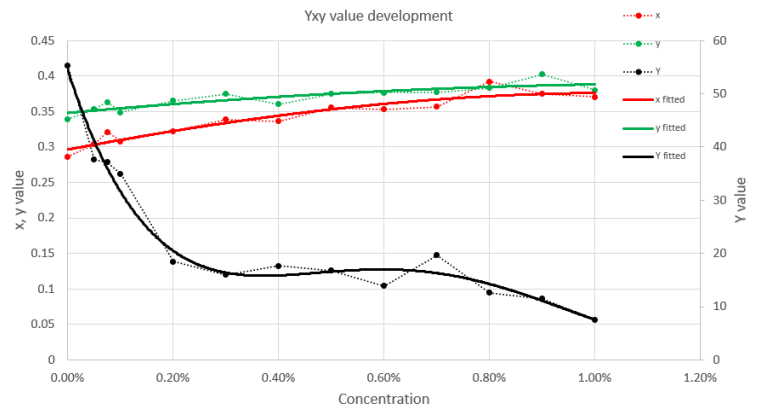
(a) RGB color code development of Fe³⁺



(b) Yxy color code development of Fe³⁺



(c) RGB color code development of S^{2-}



(d) Yxy color code development of S^{2-}

Figure 2 Color code development curve of Fe^{3+} and S^{2-} vs. concentration

2.4.2 Integration of Corrosive Water into Internal Corrosion Prediction Models (Task 3)

2.4.2.1 Theories of Electrochemical Corrosion Measurements

In Quarterly Report #7, a general method of numerically establishing the corrosion model has been reviewed for corrosive ions especially CO_3^{2-} and S^{2-} . To develop the relationship between the corrosion rate and the corrosion environments' ion concentrations, during this quarter, potentiodynamic polarization tests were performed to countify the influences on corrosion rates of steel under various sulfur corrosion environments.

As it is known, most metallic corrosion occurs via electrochemical reactions at the interface between the metal and an electrolyte solution, which usually occurs at a rate determined by a balance between opposing electrochemical reactions. One reaction is the anodic reaction, where a metal is oxidized and releases electrons. The other one is the cathodic reaction, in which a solution species (O_2 or H^+) is reduced, removing electrons from the metal. When these two reactions are in equilibrium, the flow of electrons from each reaction is balanced, which prevents the net electron flow, i.e. current. The two reactions can take place on one metal or on two dissimilar metals (or sites) that are electrically connected. A typical measurement method of this electrochemical process is the potentiodynamic polarization test [1]. Figure 3 shows a sample result of the Potentiodynamic Scanning (PDS) curve from the Potentiodynamic polarization test. The vertical and horizontal axis represents the electrical potential and the logarithm of absolute current, respectively. The theoretical current for the anodic and cathodic reactions is shown as straight lines. While, the curved line is the sum of the anodic and cathodic currents. This is the measured current when the potential of the metal is swept with the Potentiostat experimental instrument [2]. The intersection point in the curve is actually the point where the current reverses polarity as the reaction changes from anodic to cathodic, or vice versa. The intersection point is caused by plotting along a logarithmic axis. The use of a logarithmic axis is necessary because of the wide range of current values that must be recorded during a corrosion experiment. Because of the phenomenon of passivity, the current often change by six orders of magnitude during an electrochemical experiment.

The equilibrium potential assumed by the metal in the absence of electrical connections to the metal is called the open-circuit potential, i.e. E_{oc} , which is usually the first step in most electrochemical corrosion experiments. It is very important that we measure the E_{oc} and allows sufficient time for the E_{oc} to stabilize before beginning the electrochemical experiment. A stable E_{oc} is taken to indicate that the system being studied has reached "steady state", i.e., the various corrosion reactions have assumed a constant rate.

Some corrosion reactions reach steady state in a few minutes, while others may need several hours. The value of either the anodic or cathodic current at E_{oc} is called the Corrosion Current, I_{corr} . If we can measure I_{corr} , we can use it to calculate the corrosion rate of the metal. Unfortunately, I_{corr} cannot be measured directly [3]. However, it can be estimated using electrochemical techniques. In any real system, I_{corr} and Corrosion Rate are a function of many system variables including type of metal, solution composition, temperature, solution movement, metal history, and many others [4]. In practice, many metals form an oxide layer on their surface as they corrode. If the oxide layer inhibits further corrosion, the metal is said to passivate. In some cases, local areas of the passive film break down, allowing significant metal corrosion to occur in a small area, which is pitting corrosion.

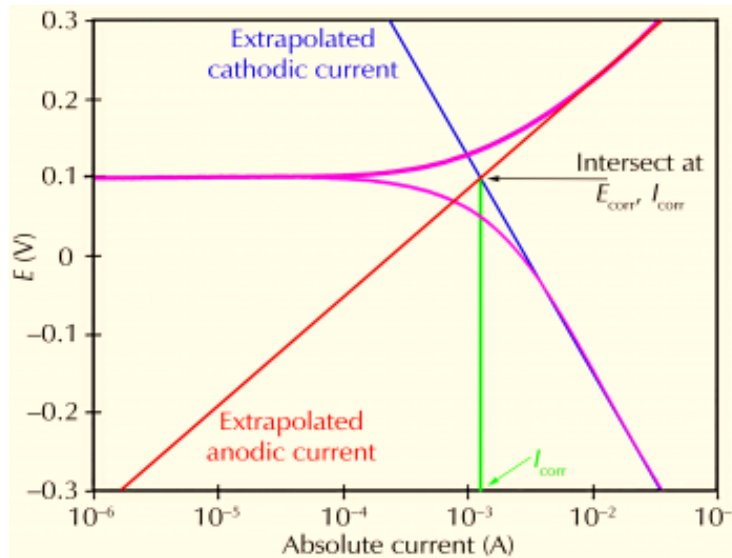


Figure 3 Typical PDS curve and Tafel Analysis

Since corrosion occurs via electrochemical reactions, electrochemical techniques are ideal for the study of the corrosion processes in this project. In electrochemical studies, a metal sample with a surface area of a few square centimeters is used to model the metal in a corroding system. The metal sample is immersed in a solution typical of the metal's environment in the system being studied. Additional electrodes are immersed in the solution, and all the electrodes are connected to potentiostat. A potentiostat allows changes in the potential of the metal sample in a controlled manner which can measure the current that flows as a function of applied potential. Since I_{corr} cannot be measured directly, an alternative way of getting is used by estimating the I_{corr} from current-versus-voltage data with the measurement of a logarithmic current versus potential curve over a range of about 0.5 volt. The voltage scan is centered on E_{oc} . A theoretical model can then be fitted from the corrosion process data [4]. Thus, the model used in this project for the corrosion process assumes that the rates of both the anodic and cathodic processes are controlled by the dynamics of the electron-transfer reaction at the metal surface, which is generally the case for corrosion reactions. An electrochemical reaction under dynamic control follows the Tafel equation (Eq.1):

$$I = I_0 e^{\frac{2.3(E-E_0)}{\beta}} \quad (1)$$

in which, I is the current resulting from the reaction, I_0 is a reaction dependent constant (Exchange Current), E is the electrode potential, E^0 is the equilibrium potential (constant for a given reaction), and β is the Tafel Constant (V/decade).

The Tafel equation, Eq. (1), describes the behavior of one isolated reaction. In a corrosion system, we have two opposing reactions: anodic and cathodic, which can be combined to generate the Butler-Volmer

Equation as below:

$$I = I_a + I_c = I_{corr} \left(e^{\frac{2.3(E-E_{oc})}{\beta_a}} - e^{\frac{2.3(E-E_{oc})}{\beta_c}} \right) \quad (2)$$

where, I is the measured current from the cell in amp, I_{corr} is the corrosion current in amp, E_{corr} is the corrosion potential in volts, β_a is the anodic β Tafel constant in volts/decade, and β_c is the cathodic.

Classic Tafel analysis is performed by extrapolating the linear portions of a logarithmic current versus potential plot back to their intersection (Figure 3). The value of either the anodic or the cathodic current at the intersection is I_{corr} . Unfortunately, many real-world corrosion systems do not provide a sufficient linear region to permit accurate extrapolation. In this project, Gamry Analysis software has been used to performs a more sophisticated numerical fit to the Butler-Volmer equation automatically. The measured data are fit to Eq. 2 by adjusting the values of E_{corr} , I_{corr} , β_a , and β_c . The curve-fitting method has the advantage that it does not require a fully developed linear portion of the curve.

2.4.2.2 Calculation of Corrosion Rate from Corrosion Current

The numerical results obtained by fitting corrosion data to a model is generally the corrosion current (I_{corr}). To convert the I_{corr} into a form of describing the corrosion rate (mm/y or min/year), conversion equation is established based on the following theory. Assume an electrolytic dissolution reaction involving a chemical species S, the electrochemical reaction can be described as:



From Faraday's Law, current flow can be presented by mass from:

$$Q = nFM \quad (4)$$

in which, Q is the charge in coulombs resulting from the reaction of S, n is the number of electrons transferred per molecule or atom of S, F is the Faraday's constant, which is 96486.7 coulombs/mole, and M is the number of moles of S involved in the reaction.

Based on the concept of equivalent weight, Eq. 5 is considered as a more efficient way of expressing of Eq. 4 as below:

$$W = \frac{EW \times Q}{F} \quad (5)$$

where, W is the mass of S consumed in the reaction.

In cases where the corrosion occurs uniformly across a metal surface, the corrosion rate can be calculated in units of distance per year. Acquiring the density of S, d, and the sample area, A, conversion from a weight loss to a corrosion rate (CR) is straightforward. If the charge is given by $Q = IT$, where T is the time in seconds and I is a current substituted in the value of Faraday's constant, Eq. 5 can be rewritten as:

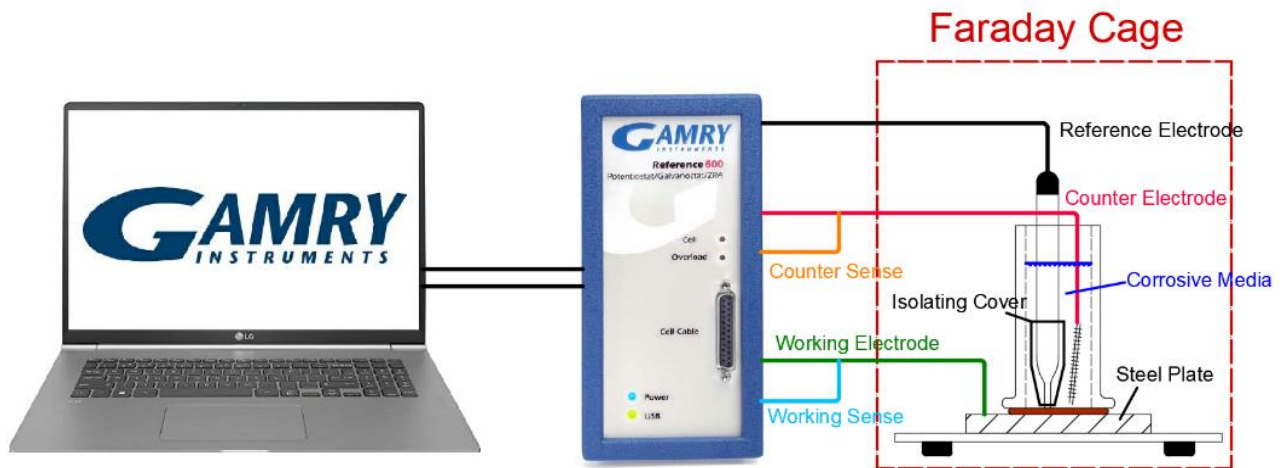
$$CR = \frac{I_{corr} K \cdot EW}{dA} \quad (6)$$

where, K is constant defines the unites for the corrosion rate which is 3272 if use mm/year (mmpy), and is 1.288×10^5 if use milli-inches/year (mpy), EW is the equivalent weight in grams/equivalent, d is the density in g/cm^3 , and A is the sample area in cm^2 .

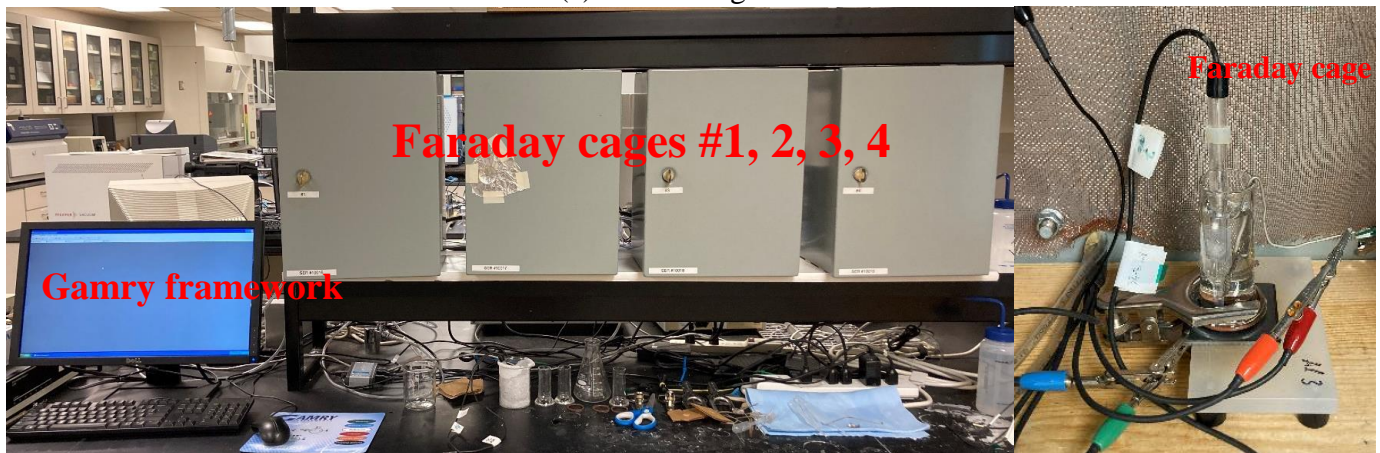
2.4.2.3 Potentiodynamic Polarization Test Setup

To gain the corrosion rate of steel under sulfur environments, sulfide solutions of different concentrations were prepared as corrosive media in potentiodynamic tests. Na_2S was used as an agent to add free S^{2-} in various dosage while not changing the pH value of the media. In addition, 3.5% Sodium Chloride solution was used as base media to provide free ion flows.

Figure 4 (a) shows the test arrangement. The test specimen is the A36 Steel plate clamped on the pilot. Both of the Reference electrode and the counter electrode are immersed in the corrosive media and been separated from each other by a plastic cover over the reference electrode. On the control end, Gamry Framework is used for data collection and preliminary data analysis. The test instrument used was Gamry Reference 600+ Potentiostat, and the sample installation is in Figure 4(b, c) with Faraday cages as a mandatory component to shield electrical interference signals. Table 2 shows all the used parameters for the performed potentiodynamic tests. Before the potentiodynamic scanning, it is suggested to test the Open Circuit Potential (E_{oc}) in order to drive the whole system into a stable status. Thus, an initial delay was set up to 1200s (20 min) to gain the E_{oc} . The Initial and Final Potential is over and below the E_{oc} by 0.3 voltage as the tested potential range. To have a more precise graphical figure, scan rate was set up to 1mV/s which is relatively low. The sample period was 1s as default. The sample area depends on the test sample and its attachments. In this test, a glass tube was used as corrosion cell with an inner bottom area 1cm², which represented the sample area. A36 steel plate has a density of 7.75-8.05g/cm³. Thus, 7.85 was determined to be the density value.



(a) Test arrangement



(b) Test instruments

(c) Sample cell installation

Figure 4 Test instrument and sample

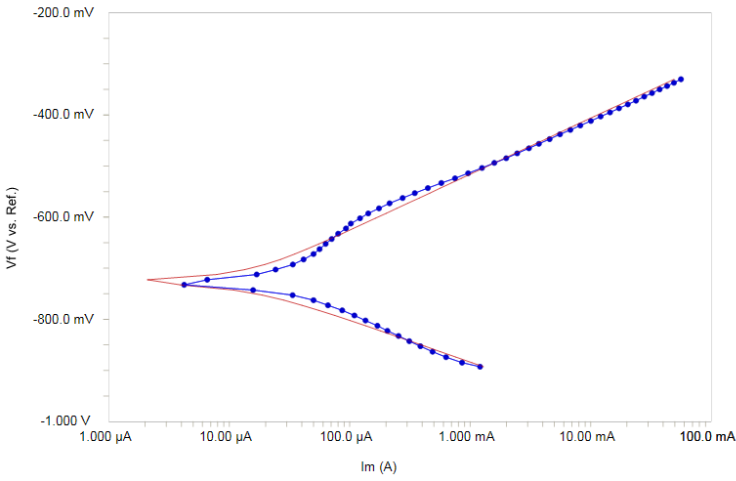
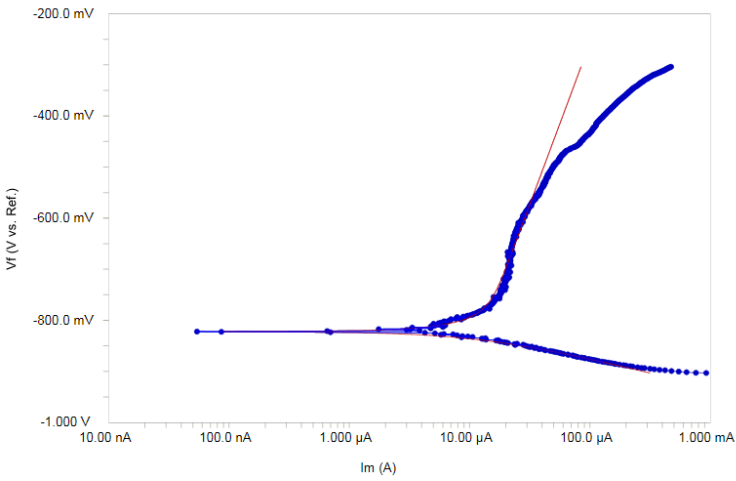
Table 2 Potentiodynamic parameter settings

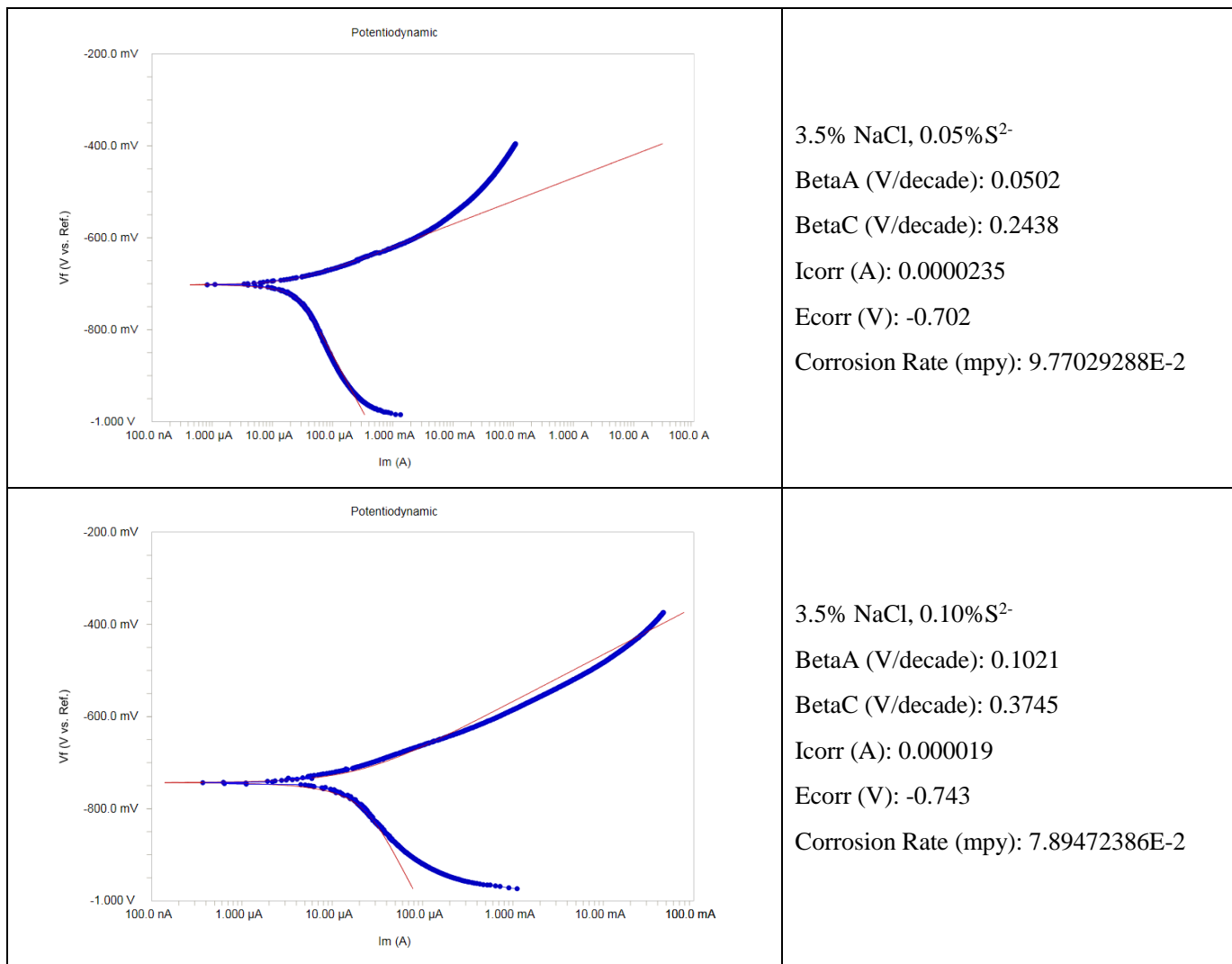
Initial E (V)	Final E (V)	Scan Rate (mV/s)	Sample period (s)	Sample Area(cm ²)	Density (g/cm ³)
0.3	-0.3	1	1	1	7.85

2.4.2.4 Preliminary Potentiodynamic Polarization Test Results

In the sensitivity tests of polymer-based colorimetric sensors of S^{2-} (Section 2.1), various concentrations have been tested includes 0.05%, 0.075%, 0.1% to 1.0%. The sensor-embedded polymer membranes showed obvious color change under different concentration conditions (Table 1). Thus, in this study, the corrosion tests were performed based on the concentrations above. Different S^{2-} concentration is achieved by adding different dosage of Na_2S into 3.5% $NaCl$ solutions which provides free ion flows. After performing the test procedure mentioned above, the Tafel figures are shown in Table 3.

Table 3 Tafel curves under experimental cases

 <p>Potentiodynamic</p> <p>Y-axis: V_f (V vs. Ref.) from -1000.0 mV to -200.0 mV X-axis: I_m (A) from 1.000 μA to 100.0 mA</p>	<p>3.5% $NaCl$, 0.00% S^{2-} BetaA (V/decade): 0.1097 BetaC (V/decade): 0.0824 I_{corr} (A): 0.0000122 E_{corr} (V): -0.726 Corrosion Rate (mmpy): 5.07519432E-2</p>
 <p>Potentiodynamic</p> <p>Y-axis: V_f (V vs. Ref.) from -1000.0 mV to -200.0 mV X-axis: I_m (A) from 10.00 nA to 1.000 mA</p>	<p>3.5% $NaCl$, 0.01% S^{2-} BetaA (V/decade): 0.632 BetaC (V/decade): 0.0575 I_{corr} (A): 0.0000128 E_{corr} (V): -0.822 Corrosion Rate (mpy): 5.31251414E-2</p>



The preliminary outcome of the Tafel curves are listed below:

- In the Tafel figures, it is seen that under the sulfur free solution environment, the corrosion rate of normal steel is 50.75 $\mu\text{m}/\text{year}$.
- Due to the increase of sulfur ions in the environment, a significant increase of the corrosion rate is observed. They rise to 53.13 $\mu\text{m}/\text{year}$, 97.70 $\mu\text{m}/\text{year}$, and 78.95 $\mu\text{m}/\text{year}$ when the sulfur ions' concentrations are 0.01%, 0.05% and 0.1%, respectively.
- The corrosion rate under 0.1% sulfur is lower than that of 0.05% sulfur condition. This phenomenon shows that the corrosion rate doesn't have a linear relationship with the increase of sulfur's concentration. More specific studies on the mechanism will be conducted in next quarter with densified tests of concentration levels of S²⁻.

2.4.3 Pipeline Inspection Robot-kit Installation and Demo Inspection Operation (Task 4)

For Task 4 (Feasibility Study of Field Installation and Inline Inspection Tools Integration), during this quarter, the research team prepared some Inspection tools along with its feasibility laboratory tests. In practical application, ILI tools, sometimes referred to as "intelligent" or "smart" pigs, is usually set up in a worm-like arrangement, consisting a flexible main body, cleaning disks, electric motors and sensors sometimes camera at its head (Figure 5). In addition to their primary function which is cleaning the debris and was deposits, it is used to inspect pipelines for evidence of internal or external corrosion, deformations, laminations, cracks, or other defects according their sensor attachments. For the purpose of

the sensors developed in this project, camera and relevant sensors are to be examined. Thus, we have chosen robot-kits with cameras to study the feasibility of camera-observation activities.

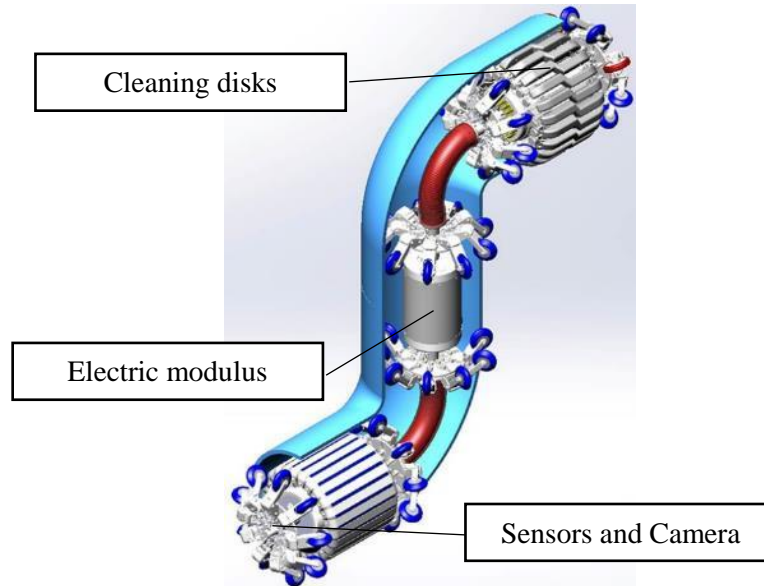


Figure 5 A Typical ILI Tool

To have the most suitable one of the field tests from maneuverability perspective, two types of Robot-car-kit were selected as ILI tools to test their performance under the designated test plans. One of them is mBot Transformable Ranger with better maneuverability because of the two track wheels. However, the disadvantage of it is the absence of built-in camera. In this case, an external Wi-Fi camera should be attached for inspection (Figure 6).

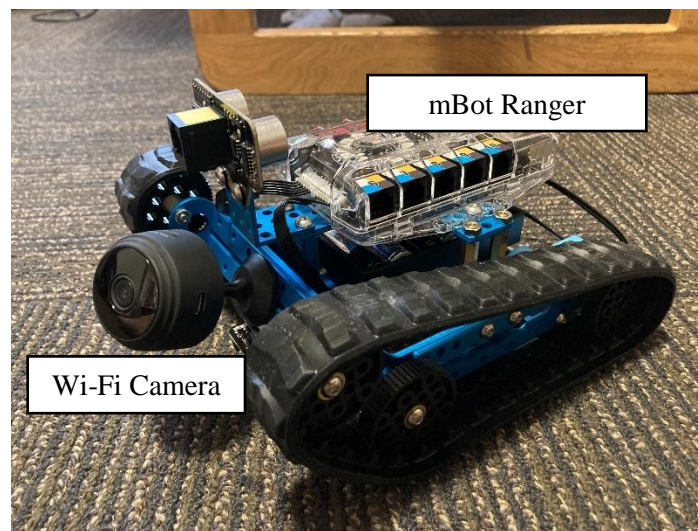
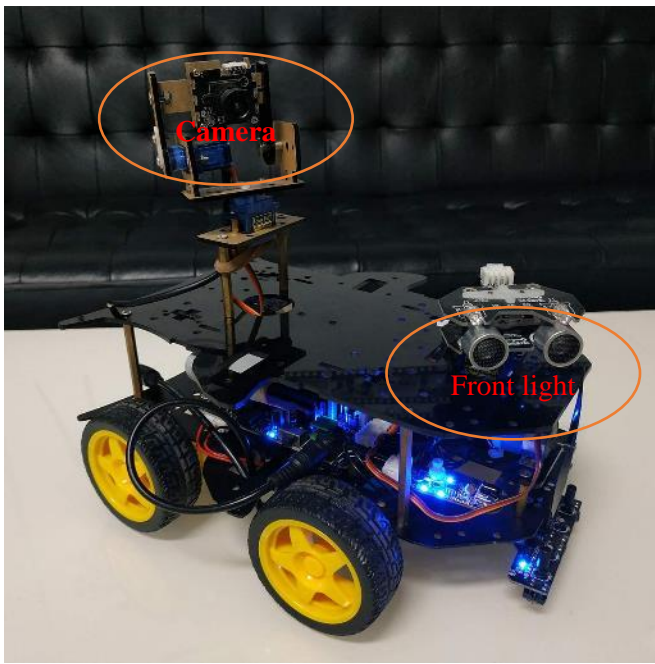
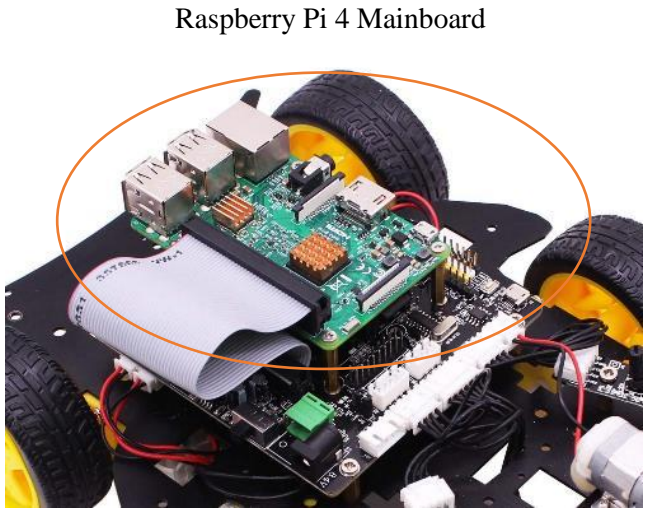


Figure 6 mBot Ranger with external camera

Another option is Yahboom Robot-Kit with an attached Raspberry Pi-4 Model B motherboard. It was chosen as the Inline Inspection Tool in this quarter, for its easier operation through mobile application. The assembled robot kit is capable for remote movement control, routine control and mark seeking. While the attached Pi motherboard is the core controller to make the car have the comprehensive function of camera, programming, and DIY (Figure 7).



(a) Yahboom Robot-Kit with camera



Raspberry Pi 4 Mainboard

(b) Raspberry Pi 4 Mainboard

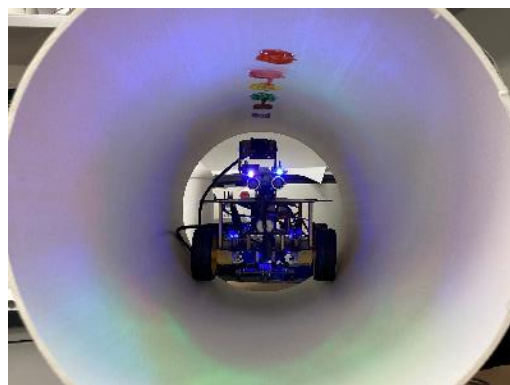
Figure 7 Camera-Robot-kit and its attachment

To validate its feasibility as an installation and inspection robot, in this quarter, a laboratory practical test was conducted. A 12” PVC pipe was prepared as test sample for the robot-kit to run through. The inner surface of the PVC pipe was marked with washable color paint to simulate the different colorimetric reaction product under various media conditions. The pipe was painted by color blue, brown, green, yellow, red and orange in sequence as shown in Figure 8 (a), and when operating the Kit run through the PVC pipe as in Figure 8 (b), a clear image from the mobile application is shown in Figure 8 (c). It is better to mention that the front light of the robot has three built-in colors as red, green and blue. Before this test, the three colors were tested individually to avoid the color temperature shift from the camera shots from human eyes. Though the results, it is found that when the LEDs are blue, the vision in the monitoring screen from mobile devices have the less color temperature shifts from bare eyes. From which it is suggested to use blue light or primarily blue as light source in dark in-line environments. This conclusion works only when adopting this particular type of Robot-kit, while it needs more verification in other circumstances.

In Figure 8 (c), a picture from the monitor screen of a working remote-control terminal, it can be seen that the graphical results given by the robot-kit is promising and reliable within an inspection procedure. Compare to Figure 8 (b), a picture directly taken from a camera, the resolution and the color saturation are basically matched with each other. This means the feasibility of the Robot-kit when representing the ILI tools performance in an in-line inspection activity. The works done on the Robot-kit is a preparation of the coming laboratory tests on the project’s objective of the sensor array’s application. The future works includes the installation and arrangement of sensor arrays, and laboratory test results of the color changes using the integrated robot kits.



(a) PVC pipe with color marks



(b) Inline Inspection using the Robot-kit



(c) Camera image from remote control device

Figure 8 Color recognition graphical results

2.5 Student Mentoring

During 2019 to 2020, four graduate students (Shuomang Shi, Ph. D. in Civil and Environmental Engineering at NDSU, Hafiz Usman Ahmed, Masters in Civil and Environmental Engineering at NDSU, and Jiapeng Lu, Ph.D. Student in chemistry at NDSU, Baiyu Jiang, Ph.D. in Civil Engineering at Rutgers University) and four undergraduate research assistants (Gina Blazanin, Alex Glowacki, Thomas Rasmussen, and Uuganbayar Ganselem) worked on this project. Currently, there are two graduate students (Shuomang Shi, Ph. D. in Civil and Environmental Engineering at NDSU, and Hafiz Usman Ahmed, Masters in Civil and Environmental Engineering at NDSU) continue working on this project. The two graduate students will continue working on this project during Quarter 9 of this project. The Ph. D. student from chemistry department of NDSU worked for the past four quarters of this project graduated, thus, in this quarter, the development of the H^+ /pH sensor was not successfully performed due to the discontinuity of the graduate students in chemistry department. Another student from chemistry department of NDSU will be hired in Quarter 9, and we will resume this subtask (H^+ /pH sensor) when the new graduate student from chemistry department is hired in next quarter. Due to the increasing risk of lab work, no undergraduate assistants were hired during this quarter or next quarter. Undergraduate research assistants will resume working for this project in Spring 2021 if it is deemed to be safe for them to work in the lab environments.

2.6 Outreach Activities

In the 2019-2020 year, the team hosted two outreach events. The first outreach event is an one-day outreach workshop named "Pipeline Challenge" workshop in BrainSTEM was conducted based on this

project on Oct. 25th, 2019. This workshop intended to let the middle school students have hands-on experiences using easy tools to plan and build pipeline, which outreached to a total of 45 middle school students. The second event is the “CORE” outreach program collaborating with CHARISM, a neighborhood-based program that works to provide opportunities to local youth and their families from low-income and refugee backgrounds to learn and connect. The workshop was planned to be eight lessons and we had six lessons to four different sites of after school programs. Unfortunately, due to COVID-19 and the widespread concern in our country and contamination, we were unable to finish out our final two lessons with CHARISM this spring after NDSU transitioned to remote learning and North Dakota public schools were suspended for the time being. The workshop was organized to be every Thursday afternoon from 3:30pm to 5:00pm starting from Feb 6th 2020. Three sites hosted elementary school students and one site hosted middle school students. In general, there are about 16 students in each site.

In the last two quarters, the team planned an outreach event of five one-day workshop to Native American high school students at five different tribal sites, collaborating with NATURE program. However, due to the compact of COVID-19, the planned outreach event to Native American community was postponed to next year due to the continuous outbreak of the pandemic for the safety concerns from the Native American community. We will report the details when it is resumed later. Outreach events will be resumed whenever it is safe to continue.

2.7 Future work

In the 9th quarter, we will continue working on all the four tasks with specially efforts focusing on the development of the H⁺/pH sensor:

- 1) Task 2.1: Develop sensor film for the H⁺/pH;
- 2) Task 2.2: Test and analyze more sensor film characteristics and continue quantify the color changes of the H⁺/pH;
- 3) Task 3: Analysis the input for the corrosion model from the sensor array color map;
- 4) Task 4: Use the robot kits for laboratory tests for the sensor array as validation and optimization.

References:

- [1] DC Electrochemical Test Methods, N.G. Thompson and J.H. Payer, National Association of Corrosion Engineers, 1440 South Creek Drive, Houston, TX 77084-4906.
- [2] Principles and Prevention of Corrosion, Denny A. Jones, Prentice-Hall, Upper Saddle River, NJ 07458 (1996). ISBN 0-13-359993-0.
- [3] Polarization Resistance Method for Determination of Instantaneous Corrosion Rates, J. R. Scully, Corrosion,56, 199 (2000)
- [4] Corrosion Testing and Evaluation, STP 1000, Edited by R. Baboian and S. W. Dean, 1991. American Society for Testing and Materials, 100 Barr Harbor Drive, West Conshohocken, PA 19428.